Detecting the Milky Way's dark disk

Bruch, T ; Read, J ; Baudis, L ; Lake, G

Abstract: In the standard model of disk galaxy formation, a dark matter disk forms as massive satellites are preferentially dragged into the disk plane and dissolve. Here, we show the importance of the dark disk for direct dark matter detection. The low velocity of the dark disk with respect to the Earth enhances detection rates at low recoil energy. For weakly interacting massive particle (WIMP) masses M WIMP gsim 50 GeV/c 2, the detection rate increases by up to a factor of 3 in the 5-20 keV recoil energy range. Comparing this with rates at higher energy is sensitive to M WIMP, providing stronger mass constraints particularly for M WIMP gsim 100 GeV/c 2. The annual modulation signal is significantly boosted and the modulation phase is shifted by 3 weeks relative to the dark halo. The variation of the observed phase with recoil energy determines M WIMP, once the dark disk properties are fixed by future astronomical surveys. The constraints on the WIMP interaction cross section from current experiments improve by factors of 1.4-3.5 when a typical contribution from the dark disk is included.

DOI: https://doi.org/10.1088/0004-637X/696/1/920

Detecting the Milky Way's Dark Disk

Tobias Bruch,* Justin Read,† Laura Baudis*, and George Lake†‡
University of Zürich, Winterthurerstrasse 190, CH-8057, Zürich, Switzerland
(Dated: November 24, 2010)

In ΛCDM, massive satellites are dragged into the disk-plane by dynamical friction where they dissolve into a stellar thick disk and a more massive dark matter disk. The distinctive kinematics of the dark disk matches the stars that also entered in the satellites. The lower velocities of the dark disk with respect to the Earth enhances detection rates at low recoil energy. For WIMP masses $\gtrsim 50\,\mathrm{GeV/c^2}$, the detection rate increases by up to a factor of 3 in the 5 - 20 keV recoil energy range. Comparing this with rates at higher energy will improve constraints on the WIMP mass, particularly for masses $\gtrsim 100\,\mathrm{GeV/c^2}$. The annual modulation signal of the dark disk is significantly boosted and its modulation phase is shifted by ~ 3 weeks relative to the dark halo. The variation of the observed phase with recoil energy can also be used to determine the WIMP mass once the dark disk properties are fixed by future astronomical surveys. The constraints on the WIMP interaction cross section from current experiments improve by factors of 1.4 to 3.5 when a typical contribution from the dark disk is included.

PACS numbers: 95.35.+d, 98.35.Ce, 98.35.Df, 98.35.Mp, 98.35.Pr

A mysterious dark matter dominates the matter content of the Universe. There are no dark matter candidates in the Standard Model of particle physics, but they are plentiful in extended models. Among these, Weakly Interacting Massive Particles (WIMPS) [1] stand out for their possible detection.

WIMPs may be detected directly by scattering in a laboratory detector [2] or indirectly by their annihilation products from regions where their densities are highest [3]. In either case, we must know the dark matter's phase space structure to predict rates. In early calculations, the Standard Halo Model (SHM) of the dark matter assumed no rotation and the density distribution was taken to be a spherical isothermal sphere with a core radius of several kpc. More recent modeling includes the cuspier central profiles from ΛCDM simulations [4], producing changes of $O(10\%)$ with respect to the SHM [5]. Larger boosts have been claimed if dark matter is highly clumped [6], but it is more likely that we live outside a clump, leading to a modest reduction in the local density [7].

Dark matter only simulations are being done at extremely high resolution, but they may not be addressing the "next to leading order" of the model. Galaxies are rich in substructure that interacts with the disk of our galaxy. Either accretion of a satellite by a thin disk or heating at early times could create the thick disks [8, 9] discovered in external galaxies nearly 30 years ago [10] and now seen in most or all disk galaxies [11]. While it is believed that disks form "from the inside out", thick disks are clearly older and can be more compact or more extended [12]. The Milky Way's thick disk has a scaleheight of 3 times the thin disk and a radial scalelength that is 40% longer [13]. One alternative to the "inside out" formation scenario is late accretion of satellites. Further evidence of accreted satellites [14] includes kinematic signatures of disrupted satellites in our galaxy [15] and the observation of at least one counter-rotating thick disk in another galaxy [16].

For over 50 years, analyses of the vertical distribution and motion of stars showed persistent evidence that roughly a third of the local disk was dark [17]. This was ~ 6 times the density of the dark halo and was generally assumed to be a baryonic form of dark matter, but it was proposed that it could be the same as the halo dark matter if a satellite had been accreted into the disk [18]. More recent analyses using Hipparcos data find evidence for far less if any unaccounted material [19], however there may be significant systematics [20].

It is now clear that some of ΛCDM's ubiquitous satellites will be drawn into disks and dissolve to form dark disks [18]. Read et al. 2008 [9] used a suite of high-resolution simulations to constrain the dark disk's expected properties. Due to the stochastic nature of structure formation, the density of the dark disk is not well constrained at present. They found a local dark disk to SHM density ratio of $\rho_\mathrm{d}/\rho_\mathrm{h} \sim 0.2 - 1$ in their few simulations. The accreted stars and dark matter have similar kinematics, with the dark disk being slightly hotter in the vertical direction, so the accreted thick disk stars are representative of the dark disk's kinematics [9]. This assumption gives a rotation lag v_{lag} of $40 - 50\,\mathrm{km/s}$ with respect to the local circular velocity, and dispersions of $(\sigma_R, \sigma_\phi, \sigma_z) = (63, 39, 39)\,\mathrm{km/s}$ [9]. However, a significant fraction of the Milky Way thick disk may also have formed through heating of an early thin disk at high redshift [8, 9]. Future surveys like RAVE [23] and GAIA [24] will measure the local dark disk to SHM density ratio $\rho_\mathrm{d}/\rho_\mathrm{h}$ and use chemical signatures of stars to disentangle accretion from heating to provide tighter constraints on the dark disk's kinematics. Current observations provide a conservative upper bound of $\rho_\mathrm{d}/\rho_\mathrm{h} < 3$ [9, 19].

*Physics Institute
†Institute for Theoretical Physics
‡Electronic address: [lake,read,lbaudis,tbruch]@physik.uzh.ch

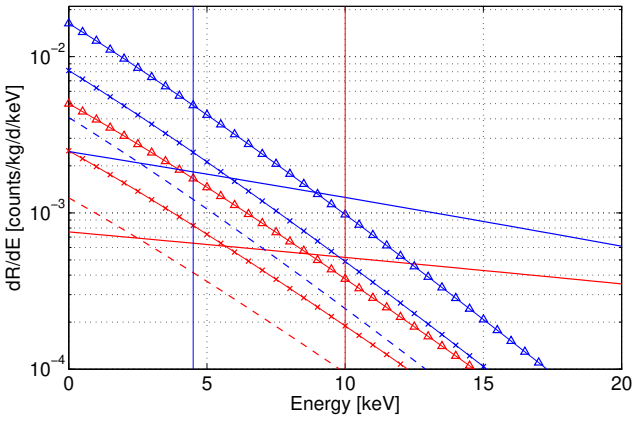

FIG. 1: Differential recoil rates for a Ge (red) and Xe (blue) target, for dark matter particles with a mass of 100 GeV/c^2 and a WIMP-nucleon cross section of $10^{-8.5}$ pb in the SHM (solid line) and in the dark disk. Three different values of $\rho_{\rm d}/\rho_{\rm h}$ (0.5 dashed, 1 $\times$ and 2 $\triangle$) are shown. Vertical lines mark current experiment thresholds: XENON10 [21] (blue) using a Xe and CDMS-II [22] (red) using a Ge target.

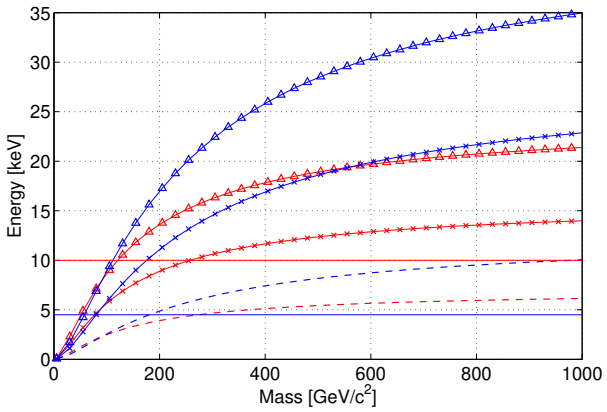

FIG. 2: The recoil energy below which the signal is dominated by the dark disk (compared to the SHM) as a function of the WIMP's mass for Ge (red) and Xe (blue) targets. Three different values of $\rho_{\rm d}/\rho_{\rm h}$ (0.5 dashed, 1 $\times$ and 2 $\triangle$) are shown. Horizontal lines mark current experiment thresholds: XENON10 [21] (blue) using a Xe and CDMS-II [22] (red) using a Ge target.

Given these uncertainties, we model the dark disk with a simple 1D Maxwellian distribution, with a dispersion and lag, $\sigma = v_{lag} = 50\,$km/s to show its general effect on direct detection. We assume a range of density ratios $\rho_{\rm d}/\rho_{\rm h} = 0.5 - 2$. The qualitative features are robust through this range.

Direct detection experiments measure nuclear recoil rates above the energy threshold in one of several detector media [25]; here we consider Ge and Xe. The energy imparted in elastic WIMP-nucleon collisions ranges from a few to tens of keV. The expected recoil rate per unit mass, unit nuclear recoil energy and unit time is [26]:

$$\frac{dR}{dE} = \frac{\rho\sigma_{\rm wn}|F(E)|^2}{2m\mu^2}\int_{v>\sqrt{ME/2\mu^2}}^{v_{max}}\frac{f(\mathbf{v},t)}{v}d^3v \qquad (1)$$

where ρ is the local dark matter density ($\rho_h = 0.3\,$GeV/cm^3 in the SHM), $\sigma_{\rm wn}$ is the WIMP-nucleus scattering cross section, $F(E)$ is the nuclear form factor, m and M are the masses of the dark matter particle and of the target nucleus, respectively, μ is the reduced mass of the WIMP-nucleus system, $v = |\mathbf{v}|$ and v_{max} is the maximal velocity in the earth frame for particles moving at the galactic escape velocity $v_{esc} = 544\,$km/s [27]. We consider only the spin-independent scalar WIMP-nucleus coupling in this paper, since it dominates the interaction (depending however on the dark matter particle) for target media with nucleon number A $\gtrsim$ 30 [28]. We model the velocity distributions of particles in the dark disk and the SHM with a simple 1D Maxwellian:

$$f(\mathbf{v},t) \propto \exp\left(\frac{-(\mathbf{v}+\mathbf{v}_\oplus(t))^2}{2\sigma^2}\right) \qquad (2)$$

where $\mathbf{v}$ is the laboratory velocity of the dark matter particle and the instantaneous streaming velocity $\mathbf{v}_\oplus = \mathbf{v}_{\rm circ} + \mathbf{v}_\odot + \mathbf{v}_{\rm orb}(t)$. This streaming velocity is the sum of local circular velocity $\mathbf{v}_{\rm circ} = (0, 220, 0)\,$km/s, the peculiar motion of the sun $\mathbf{v}_\odot = (10.0, 5.25, 7.17)$ km/s [29] with respect to $\mathbf{v}_{\rm circ}$ and the orbital velocity of the earth around the sun $\mathbf{v}_{\rm orb}(t)$.

$$v_{{\rm orb}_{\rm R}}(t) = \langle v_{\rm orb}\rangle\,(1 - e\sin(\lambda(t) - \lambda_0))\cos\beta_R\sin(\lambda(t) - \lambda_R)$$
$$v_{{\rm orb}_\phi}(t) = \langle v_{\rm orb}\rangle\,(1 - e\sin(\lambda(t) - \lambda_0))\cos\beta_\phi\sin(\lambda(t) - \lambda_\phi)$$
$$v_{{\rm orb}_z}(t) = \langle v_{\rm orb}\rangle\,(1 - e\sin(\lambda(t) - \lambda_0))\cos\beta_z\sin(\lambda(t) - \lambda_z)$$

where e is the ellipticity of the Earth's orbit, λ_0 is the longitude of the orbit's minor axis, λ_i and β_i are the ecliptic longitudes and latitudes, respectively, of the R, ϕ, z axes in galactic coordinates, $\lambda(t)$ is the time dependend ecliptic longitude and $\langle v_{\rm orb}\rangle = 29.79\,$km/s is the Earth's mean orbital velocity [26]. In the SHM, the halo has no rotation and the dispersion $\sigma = |\mathbf{v}_{\rm circ}|/\sqrt{2}$. For the dark disk, the velocity lag $\mathbf{v}_{lag} = (0, 50, 0)$ km/s replaces $\mathbf{v}_{\rm circ}$ and a dispersion of 50 km/s is adopted.

The lower relative velocities of the dark disk significantly increases the differential rate at low energies compared to the SHM rate (Fig.1). Detection of the dark disk depends crucially on the detector's low energy threshold. The differential rate for a specific WIMP target depends on the WIMP mass. In Fig. 2, we show the energy below which the dark disk dominates the rate as a function of the WIMP mass, for three values of $\rho_{\rm d}/\rho_{\rm h}$. The total rate in a detector is the sum of the two contributions from the SHM and the dark disk, which dominate at high and low energies, respectively. The details of the differential rate with energy betrays both the contribution of the dark disk relative to the SHM and the WIMP's mass. For WIMP masses $\gtrsim 50\,$GeV/c^2, the dark disk contribution lies above current detector thresholds, giving a much greater change in detection rate with recoil energy compared to the SHM alone.

The motion of the Earth around the Sun gives rise to

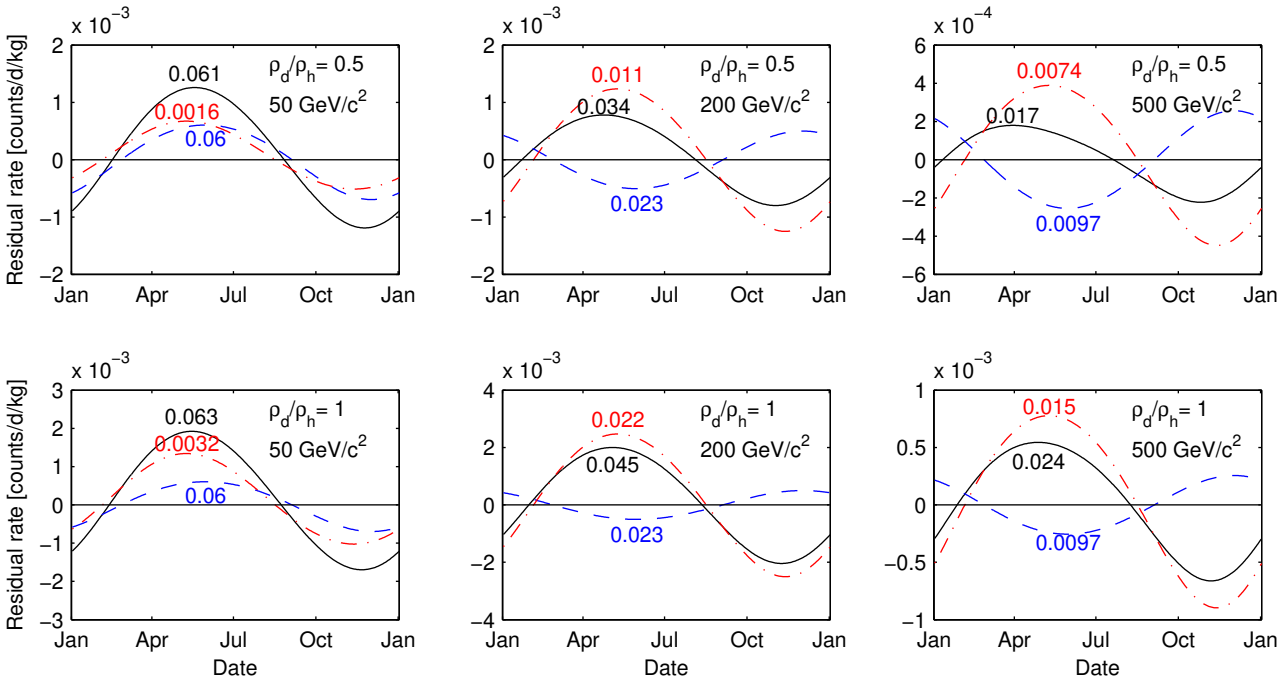

FIG. 3: The annual modulation shown as the residual counting rate versus date for the XENON10 [21] experiment (4.5 to 27 keV). The residuals are calculated with respect to the mean counting rates (given as numbers over each line) using a WIMP-nucleon cross section of 10^{-7} pb. The top/bottom row is calculated for $\rho_{\rm d}/\rho_{\rm h} = 0.5/1$ and WIMP masses (left to right) of $50\,{\rm GeV/c^2}$, $200\,{\rm GeV/c^2}$ and $500\,{\rm GeV/c^2}$. The (blue/dashed) line is the modulation signal obtained from the SHM, the (red/dot-dashed) line is the modulation signal from the dark disk and the (black/solid) line is the total modulation signal. The maximum of the dark disk contribution is shifted to May 9th compared to the SHM's maximum/minimum on May 30th.

an annual modulation of the event rate and recoil energy spectrum in a terrestrial detector [26]. The annual modulation is more pronounced for the dark disk, since the relative change to the mean streaming velocity owing to the Earth's motion is larger ($\sim$19%) compared to the SHM ($\sim$6%). Fig. 3 shows the residual integrated rates for a liquid xenon detector throughout a year, for three different WIMP masses and two values of $\rho_{\rm d}/\rho_{\rm h}$. The residuals are calculated with respect to the mean counting rates in a given energy region. The phase (defined at maximum rate) of the dark disk and the SHM differ because the Sun's motion is slightly misaligned to the dark disk. While the phase of each component does not depend on the WIMP mass, their sum does because their amplitudes depend on the WIMP mass. We show this dependency in Fig. 4, for three values of $\rho_{\rm d}/\rho_{\rm h}$. This is a new effect introduced by the presence of the dark disk that allows the WIMP mass to be uniquely determined from the phase of the modulation signal, for given $\rho_{\rm d}/\rho_{\rm h}$. Notice that there is an amplitude flip for the SHM that occurs as the WIMP mass is increased, which is not seen for the dark disk. As the WIMP mass is lowered, the "crossing energy" at which the differential rates for minimal and maximal WIMP velocity are equal shifts to lower energies. For the dark disk, it remains close to, or below, current thresholds and so the amplitude flip is not seen for WIMP masses $\lesssim 2\,{\rm TeV/c^2}$.

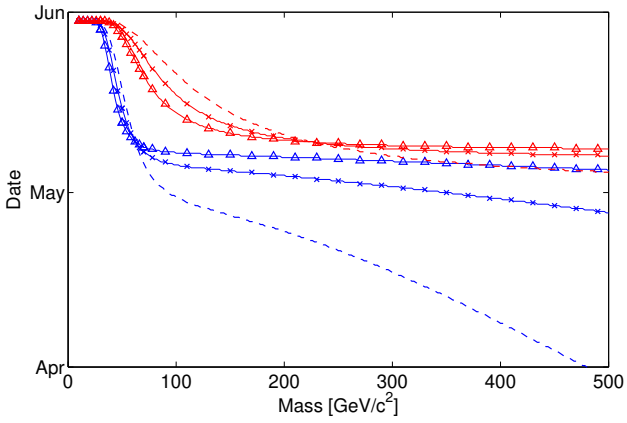

FIG. 4: Phase shifts in the energy range reported by the CDMS-II [22] experiment (10-100 keV) (red) and the XENON10 [21] experiment (4.5-27 keV) (blue), for three different values of $\rho_{\rm d}/\rho_{\rm h}$ (0.5 dashed, 1 $\times$ and 2 $\triangle$).

The effect of the dark disk on current upper limits on the spin-independent (SI) WIMP-nucleon cross section is shown in Fig. 5 for CDMS-II and XENON10 [21, 22]. Depending on $\rho_{\rm d}/\rho_{\rm h}$, we exclude new regions in the allowed parameter space for WIMP masses $\gtrsim 50\,{\rm GeV/c^2}$.

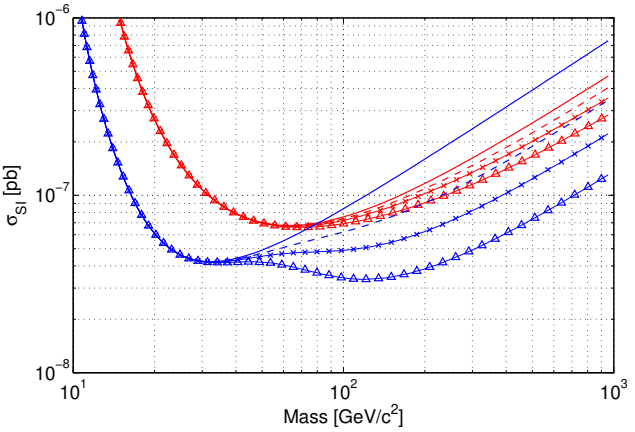

FIG. 5: Effect of the increased dark matter flux on the spin-independent WIMP-nucleon cross section constraints obtained by the CDMS-II [22] (red) and XENON10 [21] (blue) experiment for three different values of $\rho_{\rm d}/\rho_{\rm h}$ (0.5 dashed, 1 $\times$ and 2 $\triangle$).

On a final note, we find that including the dark disk component does not change the interpretation of the annual modulation signal observed in the DAMA [30] experiment for pure SI coupling. Above a WIMP mass of $10\,\mathrm{GeV/c^2}$, the allowed DAMA region is still excluded by CDMS-II and XENON10 [21, 22] results, while below $10\,\mathrm{GeV/c^2}$ no new parameter region opens.

Conclusions

In ΛCDM, a dark matter disk forms from the accretion of satellites. In this letter, we show how its lower velocities with respect to the Earth alters the expected detection rate and annual modulation signal in dark matter detectors. Our main findings are:

The dark disk boosts the detection rates at low recoil energy. For WIMP masses $\gtrsim 50\,\mathrm{GeV/c^2}$, recoil energies of 5 - 20 keV and $\rho_{\rm d}/\rho_{\rm h} \leq 1$, the rate is boosted by factors up to 2.4 for Ge and 3 for Xe targets. Comparing this with the rates at higher energy will constrain the WIMP mass, particularly for masses above $100\,\mathrm{GeV/c^2}$.

The dark disk has a different annual modulation phase than the dark halo, while the relative amplitude of the two components varies with recoil energy and WIMP mass. As a result, there is a new richness in the annual modulation signal that varies uniquely with the WIMP mass, for given dark disk properties (the properties of the dark disk will be measured from next generation surveys [23, 24]).

The increased expected dark matter flux provides new constraints on the WIMP cross section from current experiments. For likely dark disk properties ($\rho_{\rm d}/\rho_{\rm h} \leq 1$), the constraints for pure spin-independend coupling improve by up to a factor of 1.4 for CDMS-II and 3.5 for XENON10 [21, 22].

We acknowledge support from the Swiss NSF and the wonderful working environment and support of UZH.

[1] B. W. Lee and S. Weinberg, Phys. Rev. Lett., 39. 165 (1977); J. E. Gunn, B. W. Lee, I. Lerche, D. N. Schramm, and G. Steigman, ApJ, 223, 1015 (1978); J. Ellis, J. S. Hagelin, D. V. Nanopoulos, K. Olive, and M Srednicki, Nucl. Phys. B, 238, 453 (1984).

[2] M. W. Goodman and E. Witten, Phys. Rev. D, 31, 3059 (1985).

[3] J. Silk and M. Srednicki, Phys. Rev. Lett., 53, 624 (1984); G. Lake, Nature, 345, 39 (1990).

[4] J. F. Navarro, C. S. Frenk, & S. D. M. White, ApJ, 490, 493 (1997); B. Moore, F. Governato, T. Quinn, J. Stadel, and G. Lake, ApJL, 499, L5 (1998).

[5] M. Kamionkowski and A. Kinkhabwala, Phys. Rev. D, 57, 3256 (1998).

[6] A. M. Green, Phys. Rev. D, 66, 083003 (2002).

[7] M. Kamionkowski, and S. M. Koushiappas, arXiv e-prints, 0801.3269 (2008).

[8] S. Kazantzidis *et al.*, arXiv:astro-ph/0708.1949 (2007).

[9] J. I. Read, G. Lake, O. Agertz, and V. P. Debattista, arXiv:astro-ph/0803.2714 (2008).

[10] D. Burstein, ApJ, 234, 829 (1979); R. Zinn, ApJ, 241, 602 (1980); G. Gilmore and N. Reid, MNRAS, 202, 1025 (1983).

[11] P. Yoachim and J. J. Dalcanton, AJ, 131, 226 (2006).

[12] J. J. Dalcanton and R. A. Bernstein, AJ, 124, 1328 (2002).

[13] M. Jurić *et al.*, ApJ, 673, 864, (2008).

[14] G. Gilmore, R. F. G. Wyse, and K. Kuijken, Ann. Rev. Astr. Ap., 27, 555 (1989).

[15] G. Gilmore, R. F. G. Wyse, and J. E. Norris, ApJL, 574, L39 (2002); N. F. Martin *et al.*MNRAS, 348, 12 (2004).

[16] P. Yoachim and J. J. Dalcanton, ApJ, 624, 701 (2005).

[17] J. H.Oort , Bull. Astr. Soc. Neth., 6, 24 (1932) & 15, 45 (1960); J. N. Bahcall, ApJ, 287, 926 (1984).

[18] G. Lake, AJ, 98, 1554 (1989).

[19] J. Holmberg and C. Flynn, MNRAS, 313, 209 (2000).

[20] T. S. Statler, ApJ, 344, 217 (1989).

[21] J. Angle *et al.*, 2008, Phys. Rev. Lett., 100, 021303 (2008).

[22] Z. Ahmed *et al.*, arXiv:astro-ph/0802.3530v2 (2008).

[23] M. Steinmetz *et al.*, AJ, 132, 1645 (2006).

[24] M. A. C. Perryman *et al.*, A&A, 369, 339 (2001).

[25] L. Baudis, Int. J. Mod. Phys. A, 21, 1925 (2006)

[26] J. D. Lewin and P. F. Smith, Astropart. Phys., 6, 87 (1996).

[27] M. C. Smith *et al.*, MNRAS, 379, 755 (2007).

[28] G. Jungman, M. Kamionkowski and K. Griest, Physics Reports, 267, 195, (1996).

[29] W. Dehnen and J. J.Binney, MNRAS, 298, 387 (1999).

[30] R. Bernabei *et al.*, Phys. Lett. B, 480, 23 (2000).